International Journal on Emerging Technologies **11**(2): 948-953(2020)

ISSN No. (Print): 0975-8364
ISSN No. (Online): 2249-3255

Hydrodynamic Lubrication of Asymmetric Rollers by Power-Law Fluids

Swetha Lanka[1], Venkata Subrahmanyam Sajja[2] and Dhaneshwar Prasad[3]
[1]Research Scholar, Department of Mathematics, Koneru Lakshmaiah Education Foundation, Guntur-522502, India.
[2]Department of Mathematics, Koneru Lakshmaiah Education Foundation,Guntur-522502, India.
[3]Department of Mathematics, K.M. Centre for Post Graduate Studies, Lawspet, Panducherry-605008, India.

(Corresponding author: Venkata Subrahmanyam Sajja)
(Received 20 January 2020, Revised 26 March 2020, Accepted 28 March 2020)
(Published by Research Trend, Website: www.researchtrend.net)

ABSTRACT: Hydrodynamic lubrication characteristics of asymmetric rollers by power-law fluids for a heavily loaded rigid line contact system are studied in this work choosing the incompressible lubricant is to be varied with hydrodynamic pressure. The important governing equations like continuity and momentum are solved analytically under usual boundary conditions and the obtained a numerical solution using MATLAB. The velocity profiles of power-law fluids are presented and some significant changes in pressure, load, and traction are observed. The results are in good agreement with the previous findings.

Keywords: Hydrodynamic Lubrication, Non-Newtonian, Power–Law, Incompressible, Asymmetric Rollers.

I. INTRODUCTION

Hydrodynamic theory of lubrication is one of the important parts of Tribology. The theoretical study of hydrodynamic lubrication of roller bearings as received attention of many researchers because these are amenable to easy mathematical analysis. These bearings are widely used in industries for the purpose of supporting transverse loads [1].

Further, in hydrodynamic lubrication different types of lubricants are used to sustain the load of the system. The Newtonian lubricant is the simplest one which presence the linear relationship between shear stress and shear strain rate with a great no of lubricant molecule. However the non- Newtonian characteristics have also been invariably served in various lubrication problems [2]. In most of the classical problem lubricant is assumed to be Newtonian. However since the lubricant is subjected to extremely high pressure and shear stresses, heavily loaded rolling element bearings which act for a very short time, the Newtonian behavior of the lubricant ceases to exist [3]. Besides many lubricants contain high molecular weight polymers also make them strongly non- Newtonian. Hence, the effect of non- Newtonian lubricant is to be incorporated along with the effects of hydrodynamic pressure.

On the line of non- Newtonian fluids, Power-law lubricant model has got attention in the recent years because of its simplicity and potential to describe many lubricants such as silicon fluids, polymer solutions [4]. In fact this power law model characterizes to different types of non – Newtonian fluids i.e., visco-elastic and dilatants plus Newtonian as well when index of the power law model is unity [5]. Dien and Elrod (1983) examined the same non-Newtonian fluid model and developed a new numerical technique based on perturbation expansion for velocity under coquette dominated flow condition [6]. Sinha *et al*., (1983) examined a lubrication problem with squeezing motion for non-Newtonian power law lubricant [7].

Prasad *et al*., (1987) extended the same result adding thermal effects assuming the consistency of the lubricant to be varied with pressure and the mean temperature [8]. Jang *et al*., (2008) studied the EHL line contact problem and emphasized the fact that the non-Newtonian character of the lubricant must be taken in to account in order to predict the film thickness [9]. Prasad *et al.,* (2012) studied hydrodynamic lubrication of asymmetric rollers including thermal effects considering the consistency of the lubricant is to be varied with hydrodynamic pressure and mean film temperature under usual boundary conditions [10]. Sajja and Prasad (2015) dealt with the qualitative analysis of hydrodynamic lubrication of asymmetric rollers with non-Newtonian incompressible power law lubricants assuming consistency of lubricant to be varied with hydrodynamic pressure and mean film temperature under isothermal and adiabatic boundaries [11]. Revathi *et al*., (2019) studied the similar problem considering Bingham plastic fluid for a heavily loaded rigid system in which consistency of the lubricant is assumed to vary with hydrodynamic pressure under usual boundary conditions neglecting thermal effects [12].

The main aim of the present paper is to study the lubrication characteristics of asymmetric roller bearings under usual boundary conditions for a heavily loaded rigid line contact system by incompressible power-law fluids assuming the consistency of lubricant to be varied with hydrodynamic pressure.

II. MATHEMATICAL MODEL

Consider the problem of hydrodynamic lubrication of asymmetric rollers for a heavily loaded rigid line contact system in such a way that the two rollers having same radius and moving with different velocities lubricated by incompressible power- law fluids as mentioned in the Fig. 1.

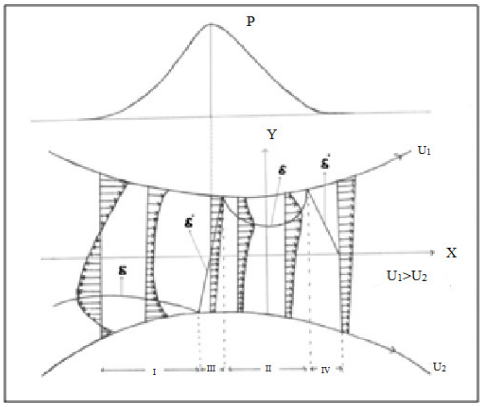

Fig. 1. Lubrications of asymmetric rollers.

Problem formulation: Consider the following momentum and continuity equations for power-law fluid model [10]

$$u_x + v_y = 0 \tag{1}$$

$$p'(x) = \tau_y \tag{2}$$

Where $\tau = m|u_y|^{n-1}u_y$ and $m = m_0 e^{\alpha p}$

The film thickness is $h = h_0 + \frac{x^2}{2R}$ with the radius R of the cylinder.

Boundary conditions [10]:

$$\left.\begin{aligned} &u = U_1,\ v = U_1\frac{dh}{dx} \quad at \quad y = h \\ &u = U_2,\ v = -U_1\frac{dh}{dx} \quad at \quad y = -h \\ &p = 0 \quad at \quad x = -\infty \\ &p = 0 \quad and \quad p'(x) = 0 \quad at \quad x = x_2 \end{aligned}\right\} \tag{3}$$

Where U_1 *and* U_2 are velocities of the rolling cylinders as shown in Fig. (1).

The velocity gradient conditions for the geometry under consideration are:

$$\frac{\partial u_1}{\partial y} \geq 0,\ \delta \leq y \leq h;\quad \frac{\partial u_2}{\partial y} \leq 0,\ -h \leq y \leq \delta;$$

$$\text{I}: -\infty < x < -x_1 \tag{4}$$

$$\frac{\partial u_3}{\partial y} \geq 0,\ -h \leq y \leq \delta;\quad \frac{\partial u_4}{\partial y} \leq 0,\ \delta \leq y \leq h;$$

$$\text{II}: -x_1 < x < x_2 \tag{5}$$

Integration of (2) for the regions: $-\infty < x < -x_1$ and $-x_1 < x < x_2$ with the help of the sign of the pressure gradients (as given in Fig. (1)) and the velocity gradient mentioned in (4), one may obtain respectively,

$$u_1 = U_1 + \left(\frac{n}{n+1}\right)\left(\frac{1}{m_1}\frac{dp_1}{dx}\right)^{1/n}\left[(y-\delta)^{\frac{n+1}{n}} - (h-\delta)^{\frac{n+1}{n}}\right],$$

$$\delta \leq y \leq h$$

$$u_2 = U_2 + \left(\frac{n}{n+1}\right)\left(\frac{1}{m_1}\frac{dp_1}{dx}\right)^{1/n}\left[(\delta-y)^{\frac{n+1}{n}} - (\delta+h)^{\frac{n+1}{n}}\right]$$

$$-h \leq y \leq \delta \tag{6}$$

$$u_3 = U_2 + \left(\frac{n}{n+1}\right)\left(-\frac{1}{m_2}\frac{dp_2}{dx}\right)^{1/n}\left[(\delta+h)^{\frac{n+1}{n}} - (\delta-y)^{\frac{n+1}{n}}\right],$$

$$-h \leq y \leq \delta$$

$$u_4 = U_1 + \left(\frac{n}{n+1}\right)\left(-\frac{1}{m_2}\frac{dp_2}{dx}\right)^{1/n}\left[(h-\delta)^{\frac{n+1}{n}} - (y-\delta)^{\frac{n+1}{n}}\right],$$

$$\delta \leq y \leq h \tag{7}$$

Volume Flux: The volume flux Q for the region: $-\infty < x < -x_1$ is obtained by $Q = \int_{-h}^{h} u\,dy$

$$Q = (U_1+U_2)h + (U_1-U_2)\delta - \left(\frac{n}{2n+1}\right)\left(\frac{1}{m_1}\frac{dp_1}{dx}\right)^{1/n} \times \left[(h-\delta)^{\frac{2n+1}{n}} + (h+\delta)^{\frac{2n+1}{n}}\right] \tag{8}$$

Similarly $Q(-x_1) = (U_1+U_2)H$ (9)

where the thickness of film H at $x = -x_1$ is considered to be $H = 1 + x_1^2$

Reynolds equation: The Pressure Reynolds equating is obtained by equating the flux (8) and (9),

$$\frac{dp_1}{dx} = m_1\left(\frac{2n+1}{n}\right)^n\left[\frac{(U_1+U_2)(h-H)+(U_2-U_1)\delta}{(h+\delta)^{\frac{2n+1}{n}} + (h-\delta)^{\frac{2n+1}{n}}}\right]^n$$

$$-\infty < x < -x_1 \tag{10}$$

$$\frac{dp_2}{dx} = -m_2\left(\frac{2n+1}{n}\right)^n\left[\frac{(U_1+U_2)(H-h)-(U_2-U_1)\delta}{(h+\delta)^{\frac{2n+1}{n}} + (h-\delta)^{\frac{2n+1}{n}}}\right]^n$$

$$-x_1 < x < x_2 \tag{11}$$

Equating u_1 *and* u_2 at $y = \delta$ and eliminating $\frac{dp_1}{dx}$ and $\frac{dp_2}{dx}$

$$(U_2-U_1)+\left(\frac{2n+1}{n}\right)\left[\frac{(U_1+U_2)(h-H)+(U_2-U_1)\delta}{(h+\delta)^{\frac{2n+1}{n}}+(h-\delta)^{\frac{2n+1}{n}}}\right]$$
$$\times\left[(h+\delta)^{\frac{n+1}{n}}-(h-\delta)^{\frac{n+1}{n}}\right]=0 \quad (12)$$

which is not valid in the neighborhood of $-x_1$

Dimensionless scheme:

$$\bar{x}=\frac{x}{R}\ ,\qquad \bar{p}=\alpha p\ ,\qquad \bar{m}=2mc_n\alpha\ ,$$

$$c_n=\frac{1}{4}\left(\frac{2n+1}{n}\right)^n\left(\frac{U}{h_0}\right)^n\left(\frac{2R}{h_0}\right),\quad \bar{h}=1+\bar{x}^2$$

$$\bar{\delta}=\delta/h_0\ ,\ \bar{U}=U_1/U_2\ ,\ \bar{h}=h/h_0\ ,\ \bar{\mu}=\bar{\mu}_0\,e^{\bar{p}}\ ,$$

$$\bar{\mu}_0=\frac{2\alpha RU}{h_0^{\,2}}\mu_0$$

Dimensionless Equations: Applying the above mentioned dimensionless scheme, the velocity Eqns. (6) and (7), pressure Reynolds equations (10) and (11), the delta equation (12) can be derived as follows:

$$\bar{u}_1=1+\left(\frac{2n+1}{n+1}\right)\left[(\bar{y}-\bar{\delta})^{\frac{n+1}{n}}-(\bar{h}-\bar{\delta})^{\frac{n+1}{n}}\right](\bar{f}_x)\ ;$$

$$\bar{\delta}\le\bar{y}\le\bar{h} \quad (13)$$

$$\bar{u}_2=\bar{U}+\left(\frac{2n+1}{n+1}\right)\left[(\bar{\delta}-\bar{y})^{\frac{n+1}{n}}-(\bar{h}+\bar{\delta})^{\frac{n+1}{n}}\right](\bar{f}_x)\ ;$$

$$-\bar{h}\le\bar{y}\le\bar{\delta} \quad (14)$$

$$\bar{u}_3=\bar{U}+\left(\frac{2n+1}{n+1}\right)\left[(\bar{\delta}-\bar{y})^{\frac{n+1}{n}}-(\bar{h}+\bar{\delta})^{\frac{n+1}{n}}\right](\bar{f}_x)\ ;$$

$$-\bar{h}\le\bar{y}\le\bar{\delta} \quad (15)$$

$$\bar{u}_4=1+\left(\frac{2n+1}{n+1}\right)\left[(\bar{y}-\bar{\delta})^{\frac{n+1}{n}}-(\bar{h}-\bar{\delta})^{\frac{n+1}{n}}\right](\bar{f}_x)\ ;$$

$$\bar{\delta}\le\bar{y}\le\bar{h} \quad (16)$$

Pressure Reynolds equations

$$\frac{d\bar{p}_1}{d\bar{x}}=\bar{m}_1(\bar{f}_x)^n\ ;\quad -\infty<\bar{x}<-\bar{x}_1 \quad (17)$$

$$\frac{d\bar{p}_2}{d\bar{x}}=-\bar{m}_2(-\bar{f}_x)^n\ ;\quad -\bar{x}_1<\bar{x}<\bar{x}_2 \quad (18)$$

Delta equation

$$(1-\bar{U})+\left(\frac{2n+1}{n}\right)\left[(\bar{h}+\bar{\delta})^{\frac{n+1}{n}}-(\bar{h}-\bar{\delta})^{\frac{n+1}{n}}\right](\bar{f}_x)=0 \quad (19)$$

which is not valid in the neighborhood of $-\bar{x}_1$

where $\bar{f}_x=\dfrac{(\bar{U}+1)(\bar{h}-\bar{H})+(\bar{U}-1)\bar{\delta}}{(\bar{h}+\bar{\delta})^{\frac{2n+1}{n}}+(\bar{h}-\bar{\delta})^{\frac{2n+1}{n}}}$

and $\bar{m}_1=\bar{m}_0\,e^{\bar{p}_1}$ etc. (18)

III. LOAD AND TRACTION

The load capacity is one of the important characteristics of loaded bearings because it provides an overall estimate of the efficiency of the bearings. Hence its calculation is very much needed. Integration of the pressure across the film thickness gives the load component W in the y-direction as

$$W=\int_{-\infty}^{x_2}p\,dx \quad (20)$$

The dimensionless load $\bar{W}=\dfrac{w\alpha}{\sqrt{2Rh_0}}$ is given by

$$\bar{W}=\int_{-\infty}^{\bar{x}_2}\bar{p}\,d\bar{x}=-\int_{-\infty}^{\bar{x}_2}\bar{x}\,\frac{d\bar{p}}{d\bar{x}}\,d\bar{x} \quad (21)$$

The traction force T_F, which decreases the efficiency of loaded bearings, and is from the integration of shear stress τ over the entire length then one may get

$$T_{Fh-}=-\int_{-\infty}^{x_2}\tau_{y=-h}\,dx;$$

and $T_{Fh+}=-\int_{-\infty}^{x_2}\tau_{y=h}\,dx$ (22)

Dimensionless tractions are given by

$$\bar{T}_{Fh-}\left(=\alpha\frac{T_{F_0}}{h_0}\right)=-\int_{-\infty}^{\bar{x}_2}\bar{\tau}_{\bar{y}=-\bar{h}}\,d\bar{x};$$

and $\bar{T}_{Fh+}=-\int_{-\infty}^{\bar{x}_2}\bar{\tau}_{\bar{y}=\bar{h}}\,d\bar{x}$ (23)

IV. RESULT AND DISCUSSION

The bearing characteristics, which specify the lubrication behavior of the system, depend on the various parameters 'n' (flow behavior index), Ū (Rolling ratio parameter). 'n' is assumed to take the values 1.15, 1.0, 0.545, 0.4 and Ū is considered to take the values 1.0, 1.2, 1.4. For the numerical calculation, the following representative values have been used:
U_2 = 400cm/s, h_0 = 4 × 10^{-4} cm, α = 1.6 × 10-9 $dyne^{-1}$ cm^2, R = 3cm.

Velocity profile: Numerically computed velocity $\bar{u}$ verses $\bar{y}$ of the lubricant at various locations of the fluid in the gap between the surfaces are depicted in Figs. (2-4) respectively for the regions before, after, and at the point of maximum pressure. The Fig. (2) represents the velocity of the fluid before the point of maximum pressure, i.e. they are like parabolas with vertices downward in the regions before the point of maximum pressure. Fig. (3) shows that the velocity of the fluid after point of maximum pressure. It can be seen from Fig. (4) that the fluid velocity at the point of maximum

pressure increases linearly as $\overline{y}$ increases. This is in good agreement with the previous findings of Revathi *et al.*, [12].

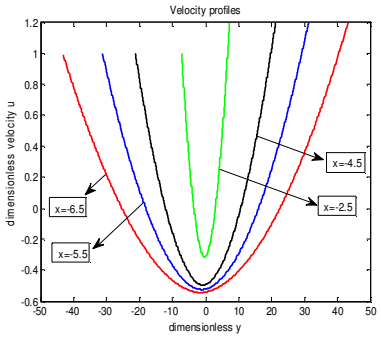

Fig. 2. Velocity at various values of x.

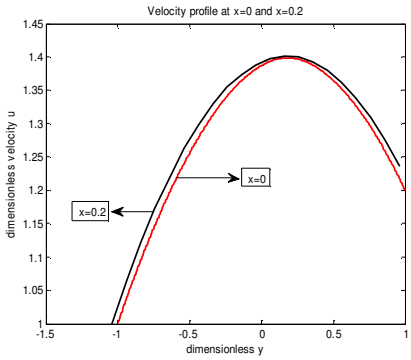

Fig. 3. Velocity at various values of x.

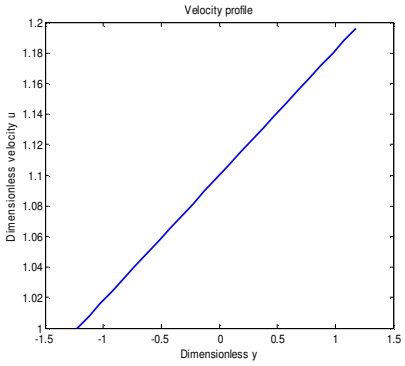

Fig. 4. Velocity at point of maximum pressure.

Pressure Distribution: The numerically computed pressure $\overline{p}$ distributions for different values of Ū and 'n' are presented in the Figs. (5) and Fig. (6) respectively. It can be observed from the Fig. (5) that the pressure $\overline{p}$ increases for fixed value of 'n=1.15' as Ū increases from 1.0 to 1.4. The same trend can be observed in previous findings of [10-12]. The pressure distribution for Ū =1.2 and for different values of 'n' is shown in Fig. (6) and can be noticed that pressure increases with 'n'. This implies that the pressure distribution for dilatant fluid is greater than that of Newtonian and pseudo-plastic fluid. This kind of trend is in good agreement with previous findings of [10-12].

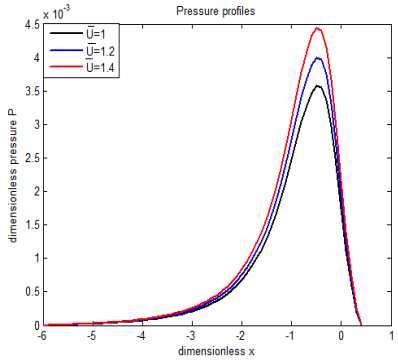

Fig. 5. Pressure profile for various values of Ū.

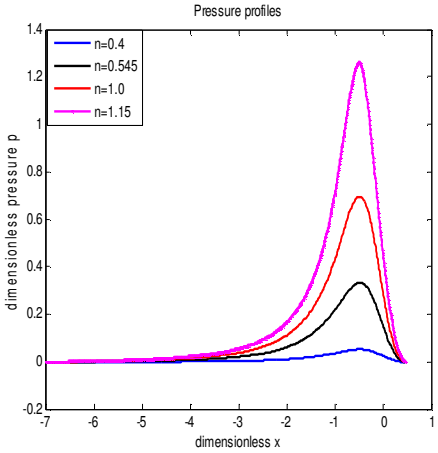

Fig. 6. Pressure profile for different values of 'n'.

Load and Traction: The dimensionless load $\overline{W}$ components for the system under consideration are presented in Fig. (7). It can be observed from the figure that the load increases with power-law index 'n' and also increases with rolling ratio parameter Ū. The dimensionless traction at both the upper and lower surfaces is calculated and presented in the Fig. (8) and Fig. (9). The traction forces are increasing with respect to both Ū and 'n' at the upper surface and this trend can be seen in Fig. (8). The traction forces are decreasing as Ū increasing at the upper surface and this trend can be seen in Fig. (9).

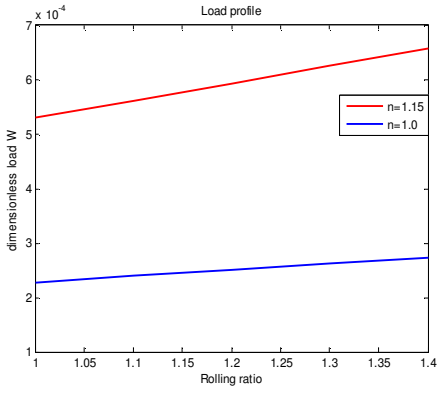

Fig. 7. Load $\overline{W}$ Profile.

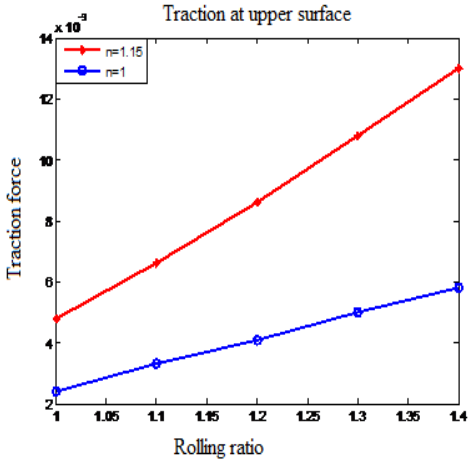

Fig. 8. Traction force at upper surface

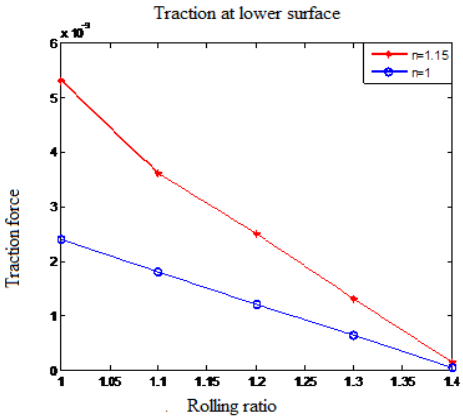

Fig. 9. Traction force at lower surface.

Delta profile: The delta is the location of the point where velocity gradient is zero. The numerically computed delta values are presented in the form of a graph in Fig. (10) and it is matching with the rough sketch presented in the Fig. (1). It is in good agreement with [13].

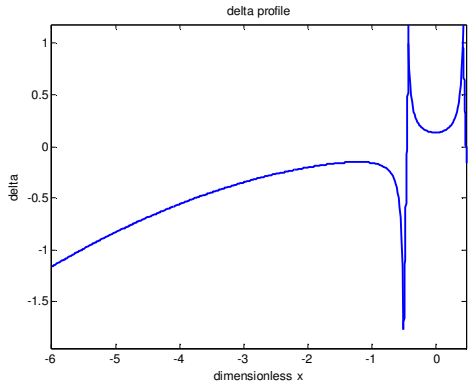

Fig. 10. Delta Profile.

Consistency Profile: The consistency relation for this problem is considered as a function of pressure and it is computed numerically and presented in the Fig. (11). Since the consistency is dependent of pressure in this problem, the graph looks like pressure profile.

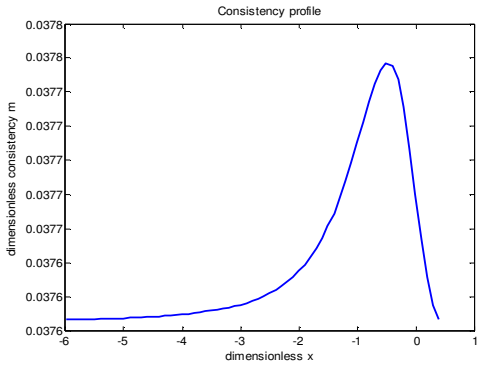

Fig. 11. Consistency Profile.

V. CONCLUSIONS

The problem has been attempted to study the hydrodynamic lubrication analysis of rolling and sliding line contact by an incompressible Power-law fluids under the usual boundary conditions. The pressure Reynolds equation and is solved for pressure, load and traction forces for various values of the sliding parameter $\overline{U}$ and the viscosity coefficient. The lubricant velocity distributions at different locations of the fluid are also discussed. The following facts may be drawn from the results obtained here:

– Velocity of the lubricant at points of maximum pressure increases linearly.

– A notable increase in lubricant pressure is observed for different values of rolling ratio Ū

– The load is found to be increasing with sliding parameter Ū and Power-law index 'n'.

– Traction forces at the upper surface are increasing with Ū and 'n'. Further, the traction forces at lower surface are found to be decreasing as sliding parameter Ū increasing.

– Since consistency is a function of pressure, the curve for consistency looks like pressure profile.

REFERENCES

[1]. Naduvinamani (2003). HDL of rough slider bearings with couple stress fluids. *Tribology International, 36,* 949-959.

[2]. Ping Huang, (2002). Study on thin film lubrication with second order fluid. *Journal of Tribology, 124,* 547-552.

[3]. Hirst, W., & Moore, A. J. (1978). EHD lubrication of pressure., *Roc. Roy. Soc. Lond.,* 403-425.

[4]. Sinha, P., & Singh, C. (1982). Lubrication of cylinder on a plane with non-Newtonian fluid considering cavition. *Journal of lubrication technology*, *104*(2), 168-172.

[5]. Chu, H. M., Li, W. L., & Chang, Y. P. (2006). Thin film elastohydrodynamic lubrication—a power-law fluid model. *Tribology International*, *39*(11), 1474-1481.

[6]. Dien, I. K., & Elrod, H. G. (1983). A generalized steady-state Reynolds equation for non-Newtonian fluids, with application to journal bearings. *Jounal of lubrication Technology, 105*(3), 385-390.

[7]. Sinha, P., Shukla, J. B., Prasad, K. R., & Singh, C. (1983). Non-Newtonian power law fluid lubrication of lightly loaded cylinders with normal and rolling motion. *Wear*, *89*(3), 313-322.

[8]. Prasad, D., Singh, P., & Sinha, P. (1987). Thermal and squeezing effects in non-Newtonian fluid film lubrication of rollers. *Wear*, *119,* 175-190.
[9]. Jang, J. Y., Khonsari, M. M., & Bair, S. (2008). Correction factor formula to predict the central and minimum film thickness for shear-thinning fluids in EHL. *Journal of tribology*, *130*(2). 024501-1 to 024501-4.
[10]. Prasad, D., Subrahmanyam, S. V., & Panda, S. S. (2012). Thermal effects in Hydrodynamic Lubrication of Asymmetric Rollers using R-K Fehlberg method. *International Journal of Engineering Science and Advanced Technology*, *2*(3), 422-437.
[11]. Sajja, V. S., & Prasad, D. (2015). Characterization of lubrication of asymmetric rollers including thermal effects. *Industrial Lubrication and Tribology, 67*(3), 246–255.
[12]. Revathi, G., Sajja, V. S., & Prasad, D. (2019). Thermal Effects in Power-Law Fluid Film Lubrication of Rolling/Sliding Line Contact. *International Journal of Innovative Technology and Exploring Engineering, 8*(9), 277-283.
[13]. Prasad, D., Subrahmanyam, S. V., & Panda, S. S. (2014). Thermal, Squeezing and compressibility effects in lubrication of Asymmetric rollers. *Tribology in Industry*, *36*(3), 244-258.

How to cite this article: Lanka, S. Sajja, V. S. and Prasad, D. (2020). Hydrodynamic Lubrication of Asymmetric Rollers by Power-Law Fluids. *International Journal on Emerging Technologies, 11*(2): 948–953